J. Mater. Environ. Sci. 4 (4) (2013) 510-519
ISSN : 2028-2508
CODEN: JMESCN

Effect of Corrosive Solution Motion on Copper – Nickel Alloy Pipe in Presence of *Naphthylamine* as a Corrosion Inhibitor

Anees A. Khadom
Chemical Engineering Department - College of Engineering – Daiyla University – Baquba City 32001, Daiyla governorate, Iraq.

Received 24 Dec 2012, Revised 11 Feb 2013; Accepted 11 Feb 2013
Email address: aneesdr@gmail.com , mobile: 00964 790 2305786.

Abstract
The corrosion of copper – nickel alloy in hydrochloric acid was investigated at different temperatures, inhibitor concentrations and corrosive solution velocities. Weight loss technique was used to evaluate the corrosion rate data. *Napththylamine* was used as organic corrosion inhibitor, while hydrochloric acid was the corrosive solution. Different parameters, such as inhibitor efficiency, activation energy were obtained. Corrosion rate increased with both temperature and acid velocity, while it decreased with increases of *Napththylamine* concentration. Maximum inhibitor efficiency was at lower level of temperature, acid velocity and higher level of inhibitor concentration. Theoretical Quantum chemical calculations were used successfully to confirm the practical studies.

Keywords: Corrosion, organic inhibitor, copper – nickel alloy, acid solution, Quantum chemical.

1. Introduction
Chemical and petrochemical equipments, such as pipes, were subject to stirring rate of acids during the removal of scales and deposits. These acids, such as hydrochloric acid, may cause corrosion problem after de -scaling processes. Various attempts have been made to prevent or retard the destructive effect of corrosion on metals and alloys. Using inhibitors is one of the most practical methods for protecting metals against corrosion, especially in acidic media [1 - 4]. Among numerous inhibitors, N-heterocyclic compounds are considered to be the most effective corrosion inhibitors [5]. Up to now, various N-heterocyclic compounds are reported as good corrosion inhibitors for steel in acidic media, such as imidazoline derivatives [6,7], amines derivatives [8, 9], amino acids [10]. Generally, N-heterocyclic compounds exert their inhibition by adsorption on the metal surface through N heteroatom, as well as those with triple or conjugated double bonds or aromatic rings in their molecular structures. Furthermore, the adsorption of inhibitor on metal/solution interface is influenced by the chemical structure of inhibitor, the nature and charged surface of metal, the distribution of charge over the whole inhibitor molecule and the type of aggressive media. The aim of present paper was to study the effect of temperature and velocity on the corrosion of copper – nickel alloy in hydrochloric acid in presence of *Napththylamine* as a corrosion inhibitor.

2. Experimental work
Napththylamine (NA) was used in our previous work to prevent the corrosion of copper alloy in static conditions [11]. In present work; the corrosion behavior of copper-nickel alloys, which used widely in many industrial equipments, was studied using weight loss in absence and presence *Napththylamine* (NA) in 5% HCl solution at different temperature (35, 45, and 55 ^{o}C), different velocities (100, 200 and 300 rpm) and different inhibitor concentrations (0.01 and 0.1 M). Ring shape specimen of Cu-Ni alloy with dimension (2.22 cm) outside diameter, (1.5 cm) width, and (0.13 cm) thickness, exposing a surface area of about (10 cm^2) to

corrosive media. The corrosive HCl solution used in present work was locally produced and supplied by AL-Furat Company for Chemicals Industries - Iraq, which was diluted from 32.5% using distilled water to obtain the required concentration of 5%. The dilution was done according to well-known dilution law [12].

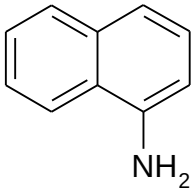

Napththylamine (NA)

Specimens were washed by detergent and flushed by tap water followed by distilled water, degreased by analar benzene and acetone, then annealed in vacuums to 600 ^{o}C for one hour and cooled under vacuum to room temperature. Before each run, specimens of Cu-Ni were abraded in sequence using emery paper of grade number 220,320, 400, and 600, then washed by running tap water followed by distilled water then dried by clean tissue, degreased with benzene, dried, degreased with acetone, dried, and finally left in desicater over silica gel. Weighing the specimen was carried out using 4 decimals digital balance and its dimensions were measured with vernier. The metal samples for weight loss runs were completely immersed in 250-cm^3 solution of corrosive solution contained in a conical flask. They were exposed for a period of three days at a desired temperature, acid concentration, and inhibitor concentration. Weight losses were determined in absence and presence of inhibitors. The data are expressed as mass loss per unit time per unit area; in the present work the units of corrosion rate were g/m^2.day (gmd). The chemical compositions of Cu-Ni alloy were (0.148 %Sn, 0.2%Fe, 0.134%Zn, 0.015%Al, 0.0003%P, 0.5%Sb, 0.0583%Pb, 0.0202%Si, 0.017%S, 0.0056%As, 10%Ni, and the reminder is Cu).

3. Results and discussions

3.1 Corrosion rate data

Table 1 shows the corrosion rate data of Cu – Ni alloy obtained at different temperature and acid velocities in absence and presence of 0.1 and 0.01 M *Naphthylamine* as a corrosion inhibitor. Corrosion rates were obtained by the following equation [13]:

$$CR = \frac{weight\ \ loss\ \ (g)}{Area\ \ (m^2) \times Time\ \ (day)} \qquad 1$$

From the corrosion rate, the percentage inhibition efficiency was calculated using the following equation:

$$IE\% = \frac{CR_{uninibit} - CR_{inhibit}}{CR_{uninhibit}} \times 100 \qquad 2$$

where $CR_{uninhibit}$ and $CR_{inhibit}$ are the corrosion rates in the absence and presence of inhibitor respectively. It is clear from Table 1 that the corrosion rate increased with both temperature and acid velocity, while it decreased with inhibitor concentration. Maximum inhibitor efficiency was 66 % at 0.1 M inhibitor efficiency, 100 rpm velocity and 35 ^{o}C. While the minimum value was 25 % at 0.01 M inhibitor efficiency, 300 rpm acid velocity and 55 ^{o}C.

1.1 Effect of temperature and activation energy

Temperature has a great effect on the rate of metal electrochemical corrosion. In case of corrosion in a neutral solution (oxygen depolarization) the increase in temperature has a favorable effect on the overpotential of oxygen depolarization and the rate of oxygen diffusion but it leads to a decrease of oxygen solubility. In case of corrosion in an acidic medium (hydrogen depolarization), the corrosion rate increases exponentially with temperature increase because the hydrogen evolution overpotential decreases [14]. The effect of temperature and Activation parameters for some systems can be estimated from an Arrhenius-type plot equation [15].

$$CR = A\ Exp\left(-\frac{E}{R\ T}\right) \qquad 3$$

Where, CR is corrosion rate, A is modified frequency factor (pre-exponential factor), E is activation energy (J/mole), R is gas constant (8.314 J/mole.K), and T is absolute temperature (K). Equation 3 was written in linear form as:

$$\ln CR = \ln A - \frac{E}{R\,T} \qquad 4$$

The plot of ln CR versus reciprocal of absolute temperature, 1/T, gives a straight line with slope equal to -E/R, from which the activation energy for the corrosion process can be calculated. The Arrhenius plots for the corrosion of Cu – Ni alloy in the hydrochloric acid containing inhibitor are shown in Fig. 1. From Table 2 it is seen that the value of activation energy (E) for the corrosion of the alloy in the HCl acid solution in the presence of the inhibitor is higher than that in the absence of the inhibitor. Also, the extent of increase is proportional to the inhibitor concentration, indicating that the energy barrier for the corrosion reaction increases with the increase in the concentration of inhibitor.

Table 1: Effect of velocity, inhibitor concentration and temperature on the corrosion of Cu-Ni in 5% HCl solution in absence and presence of inhibitor.

No	C (M)	T (^{o}C)	V (rpm)	C_R (gmd)	IE%
1	Nil	35	100	75.503	0
2			200	93.61	0
3			300	98.23	0
4		45	100	90.98	0
5			200	188.73	0
6			300	222.35	0
7		55	100	199.54	0
8			200	250.11	0
9			300	310.91	0
10	0.01	35	100	35.75	50
11			200	49.83	45
12			300	58.09	39
13		45	100	46.27	48
14			200	110.24	39
15			300	151.35	31
16		55	100	111.83	41
17			200	165.99	32
18			300	225.68	25
19	0.1	35	100	15.21	66
20			200	27.43	54
21			300	32.68	47
22		45	100	25.15	55
23			200	68.55	43
24			300	88.91	38
25		55	100	67.27	48
26			200	93.76	42
27			300	134.47	33

The increase in the activation energy E may be considered to be due to the physical adsorption of the inhibitor, which results in the increase in surface coverage with the increase in the concentration of the inhibitor. The values at different temperatures also reveal that the inhibition efficiency decreases with the increase in temperature. This may be due to the decrease in the adsorption of the inhibitor on the alloy surface as the temperature increases and a corresponding increase in the corrosion rate due to the greater area of metal being

exposed to the acid [16]. Also, activation energy decreased as acid motion increased, this may be attributed to the removal of inhibitor layer from metal surface which facilities the corrosion reaction.

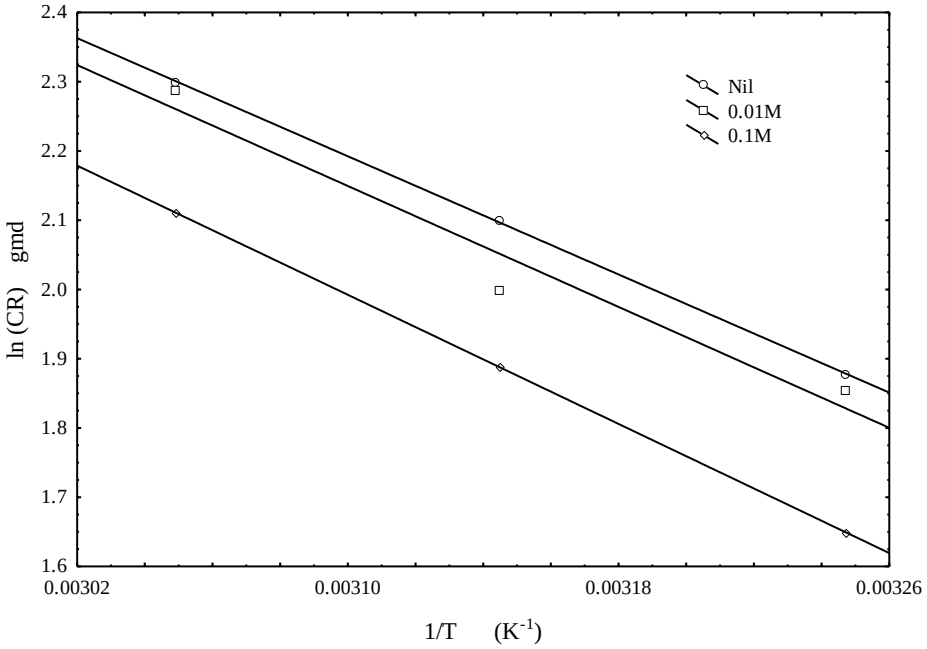

Fig. 1 Arrhenius plot at 100 rpm.

Table 2: Arrhenius parameters at different conditions.

Inhibitor conc. M	Velocity (rpm)	Activation energy (kJ/mol)
0	100	17.73
0.01		18.82
0.1		19.37
0	200	16.42
0.01		17.11
0.1		17.97
0	300	14.36
0.01		15.58
0.1		16.66

1.2 Effect of inhibitor concentration

The adsorption of inhibitor at metal/solution interfaces can markedly change the corrosion resisting properties of metals. The efficiency of organic molecules as good corrosion inhibitors mainly depends on their adsorption ability on the metal surface. So, the investigation of the relation between corrosion inhibition and adsorption is of great importance. The surface coverage *(θ=IE%/100)* data are very useful while discussing the adsorption characteristics. When the fraction of surface covered is determined as a function of the concentration at constant temperature, adsorption isotherm could be evaluated at equilibrium condition [17]. The values of θ can be used to determine the thermodynamic parameters and the mode of the adsorption process. Three adsorption isotherm were used to explain the adsorption mechanism. Langmuir [18], Frendlich [19, 20] and Flory – Huggins [20, 21]. The equations of these isotherms were fed to computer program to test the validity. The best fitting was obtained with Flory–Huggins equation. Flory – Huggins adsorption isotherm [21] can be illustrated by following equation:

$$\frac{\theta}{x(1-\theta)^x} = K_{ads}C \quad (5)$$

This model based on the principle of adsorption of organic inhibitors at the metal/solution interface takes place through the replacement of water molecules by organic inhibitor molecules according to following process [16].

$$Org_{sol} + x\, H_2O_{ads} \leftrightarrow Org_{ads} + x\, H_2O_{sol} \quad (6)$$

where Org(sol) and Org(ads) are organic molecules in the solution and adsorbed on the metal surface, respectively. K_{ads} is the adsorption constant, C is inhibitor concentration, and *x* is the number of water molecules replaced by the organic molecules. The values of K_{ads} are in relation with temperature by the following equation [21]:

$$K_{ads} = \frac{1}{55.55}\exp\left(-\frac{Q^o_{ads}}{RT}\right) \quad (7)$$

Where $\left(Q^o_{ads}\right)$, the standard adsorption free energy, 55.55 are the concentration of water in solution expressed in M, R is gas constant, and T absolute temperature. Equation 7 can be combined with equation 5 to yield the following equation:

$$\frac{\theta}{x(1-\theta)^x} = \frac{1}{55.55}\exp\left(-\frac{Q^o_{ads}}{RT}\right)C \quad (8)$$

Nonlinear estimation regression method was used to evaluate the constants of equation 8. Estimation method was done using *STATISTICA* software computer program, which produce the following equation with 0.87 correlation coefficient:

$$\frac{\theta}{0.95(1-\theta)^{0.95}} = \frac{1}{55.55}\exp\left(-\frac{17.66}{RT}\right)C \quad (9)$$

The average value of x is near unity (x= 0.95), which indicates that inhibitor molecules remove one water molecules from metal surface and the inhibitor forms monolayer on metal surface. The average value of Q_{ads} was – 17.66 kJ/mol. The value of Q_{ads} was negative this indicates that the process under study is spontaneous [22]. Generally, value of Q_{ads} up to -20 kJ.mol^{-1} is consistent with electrostatic interaction between the charged molecules and the charged metal (physisorption) while those around -40 kJ.mol^{-1} or higher than that are associated with chemisorptions as a result of sharing or transferring of electrons from the organic molecules to the metal surface to form a coordinate type of bond [23]. It is well known that decrease in efficiency with the increase of temperature is attributed to the physical adsorption. The time gap between the process of adsorption and desorption of inhibitor molecules over the metal surface is becoming shorter with increase in the temperature. Hence, the metal surface remains exposed to the acid environment for longer period, therefore the inhibition efficiency falls at elevated temperature. The inhibitor efficiency decreased with velocity increasing, this may be attributed to the separation of protective layer with velocity increasing.

1.3 Effect of velocity

The corrosion rates of Cu-Ni alloy in 5% HCl solution are determined at different velocities, temperatures and inhibitor concentrations. Table 1 shows that as the velocity increased, the corrosion rate also increased at different conditions. The effect of flow on the corrosion rate of copper has been used in a number of instances to determine if corrosion is under activation, diffusion, or mixed control. It was shown that the linear increasing of corrosion rate with velocity indicate that the corrosion process under diffusion control, while the slightly increasing indicate the mixed control process, and no effect of velocity for activation control process. Figure 2 shows the effect of velocity on corrosion rate in absence of inhibitor which reflects the mixed control corrosion process. As temperature increased the effect of speed of rotation on corrosion process increased. The same behavior observed in presence of inhibitors. The increase in fluid flow generally increases metal total weight loss by supplying the corrosives at faster rates. Relative metal/environment motion thins the quiescent layers at the metal leading to less restriction of corrosives by diffusion process. When velocity becomes extremely high mechanical effects add to corrosion and increase the damage to metals (i.e. Erosion).

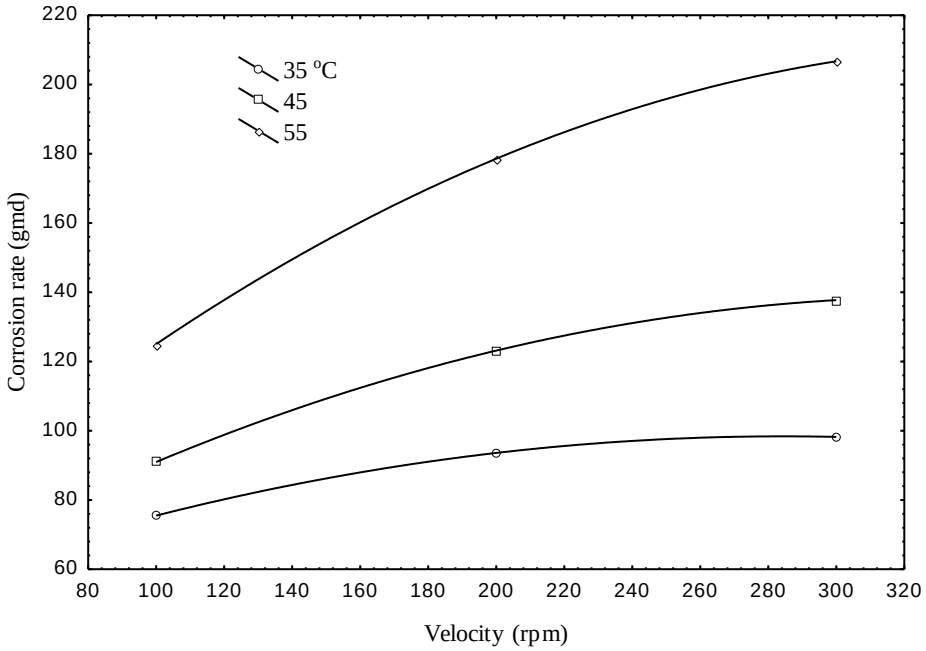

Fig. 2. Predicted corrosion rate by equations 10 and 11 against experimental one.

1.4 Mathematical models

The experimental corrosion rate results in uninhibited and inhibited 5% HCl acid as a function of temperature, velocity and inhibitor concentration are given in Table 1. Second order polynomial model and exponential model were used to represent these variables. These models take into account the effect of temperature, inhibitor concentration, velocity and the interaction of them on corrosion rate. The first second order model was:

$$C_R = \mathrm{B}_o + \mathrm{B}_1 T + \mathrm{B}_2 T^2 + \mathrm{B}_3 T\,C + B_4 C + \mathrm{B}_5 C^2 + B_6 V + B_7 V^2 + B_8 V\,C + B_9 V\,T \qquad 10$$

Another second exponential model was also suggested, which based on following assumptions:-

1. The corrosion rate results can be related to temperature by Arrhenius type, which give an indication that the corrosion rate depend exponentially on temperature reciprocal:

   $$C_R \propto \exp\left(-\frac{1}{T}\right)$$

2. The corrosion rate decreases as the inhibitor concentration increased and as acid velocity decreased, so;

   $$C_R \propto \frac{V^{B_{11}}}{C^{B_{12}}}$$

These two assumptions yield to suggest the second exponential model:

$$C_R = B_{10} V^{B_{11}} C^{-B_{12}} \exp\left(-\frac{B_{13}}{T}\right) \qquad 11$$

Where CR, T, C and V are corrosion rate ($g.m^{-2}.h^{-1}$), temperature (K), inhibitor concentration (M) and velocity (rpm) respectively. Nonlinear least squares regression analysis based on *Levenberg–Marquardt* estimation method can be used for estimation of coefficients B_o, B_1, … B_{11}, producing the following equation for Cu – Ni alloy with 0.9854 correlation coefficient for first model (eq. 10):

$$CR = 1808.76 - 15.477\,T + 0.031\,T^2 - 27.968\,T\,C + 8669.09\,C - 773.43\,C^2 - 5.263\,V - 0.001\,V^2$$

$$-1.56\,V\,C - 0.019\,V\,T$$

And another estimated model (eq.11) with 0.9286 correlation coefficients:

$$C_R = 5\times10^7 V^{0.5} C^{-0.01} \exp\left(-\frac{4940}{T}\right)$$

Fig. 3 shows predicted corrosion rate by equations 10 and 11 against experimental one. This figure shows that the both models represent the corrosion rate data with high correlation coefficients.

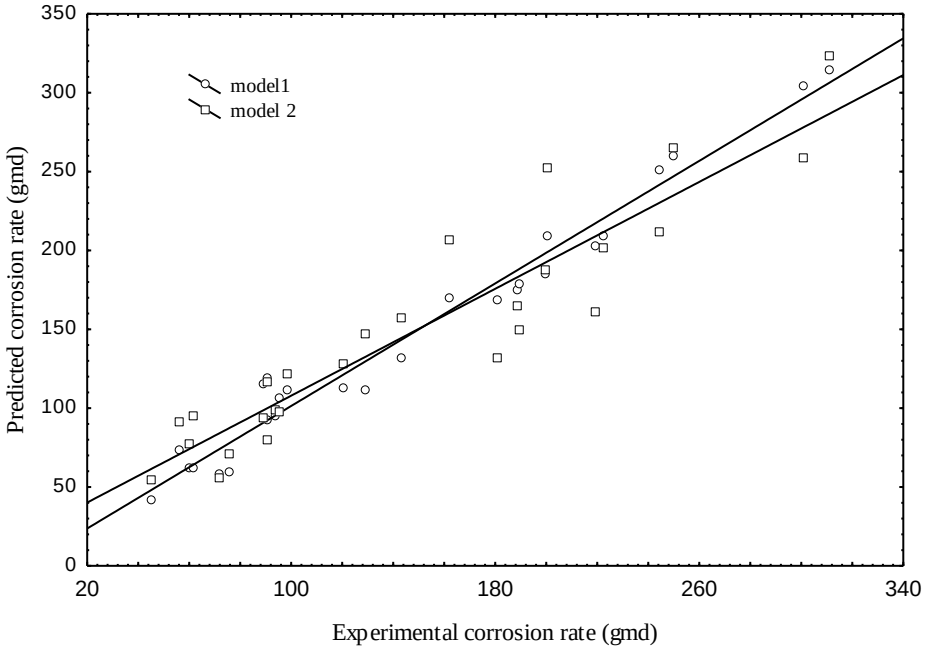

Fig. 3 Predicted corrosion rate by equations 10 and 11 against experimental one.

1.5 Mechanism of copper corrosion

The cathodic reaction that occurs on the copper alloy surface in 1.5 M HCl is the oxygen reduction, Since Cu is nobler than H^+ in the electromotive series, and a cathodic reaction other than the displacement of H^+ must account for metal dissolution. This is readily available in terms of O_2 reduction from solution [24]. Anodic dissolution of copper in chloride media has been studied extensively [25–29]. The accepted anodic reaction is the dissolution of copper through oxidation of Cu to Cu^+:

$$Cu \rightarrow Cu^+ + e \qquad 12$$

Then Cu^+ reacts with chloride ion from the solution to form CuCl:

$$Cu^+ + Cl^- \rightarrow CuCl \qquad 13$$

Insoluble CuCl precipitates on the copper surface. The CuCl species has poor adhesion, is unable to produce enough protection for the copper surface, and transforms to the sparingly soluble cuprous chloride complex, $CuCl^-_2$ [30]

$$CuCl + Cl^- \rightarrow CuCl_2^- \qquad 14$$

It has also been reported that the $CuCl^-_2$adsorbed on the surface dissolves by further oxidation [30]:

$$CuCl_{2,ads}^- \rightarrow Cu^{++} + 2Cl^- + e \qquad 15$$

It is reported that the anodic dissolution of copper in the acidic chloride solution is controlled by both electro dissolution of copper and diffusion of $CuCl^-_2$to the solution bulk [29, 30]. The cathodic corrosion reaction in an aerated acidic chloride solution is:

$$4H^+ + O_2 + 4e^- \rightarrow 2H_2O \qquad 16$$

The total corrosion reaction of copper in acidic chloride solutions is as follows:

$$2Cu + 4H^+ + 4Cl^- + O_2 \rightarrow 2Cu^{2+} + 4Cl^- + 2H_2O \qquad 17$$

1.6. Theoretical quantum chemical calculations

Quantum chemical calculations are proven to be a very powerful tool to understand the inhibition mechanism and to emphasis the experimental data [31, 32]. Through the method of quantum chemical calculations, the structural parameters, such as the frontier molecular orbital (MO), HOMO (highest occupied molecular orbital), LUMO (lowest unoccupied molecular orbital) and dipole moment (μ) were calculated. The structure of inhibitor was optimized by ArgusLab 4.0.1 package. The quantum chemical parameters were estimated by PM3 method. The optimized minimum energy geometrical configurations of test compounds are given in Fig. 4, A. The computed quantum chemical parameters like energy of highest occupied molecular orbital (E_{HOMO}), energy of lowest unoccupied molecular orbital (E_{LUMO}), HOMO–LUMO energy gap and dipole moment are summarized in Table 3. It has been well documented in literature that [33] higher the value of E_{HOMO} of the inhibitor, greater is the ease of inhibitor to offer electrons to unoccupied d orbital of metal atom and higher is the inhibition efficiency of the inhibitor. Further lower the E_{LUMO}, easier is the acceptance of electrons from metal atom to form feedback bonds. The gap between HOMO–LUMO energy levels of molecules was another important parameter that needs to be considered. Smaller the value of ΔE of an inhibitor, higher is the inhibition efficiency of that inhibitor [34]. The Mulliken charge distributions of the inhibitors are presented in Table 4. It can be readily observed that nitrogen atoms and some carbon atoms have higher charge densities. The regions of highest electron density are generally the potential sites for the electrophiles attacked [35, 36]. The use of Mulliken population analysis to probe adsorption center of inhibitors has earlier been reported [37]. Based on the calculations, the highest electron densities were located on N and C atoms implied that the N and C atoms were the active centers, which have the strongest ability of bonding to the metal surface. On the other hand, HOMO (Fig. 4, B) was mainly distributed on the area containing carbon and nitrogen atoms and this area is probably the primary site of the bonding. It was found that these amines inhibitors apart from existing in the cationic form can also interact with metal surface through the electrostatic attraction. This interaction with the metal surface with several numbers of active centers is forming a protective layer on the copper alloy surface.

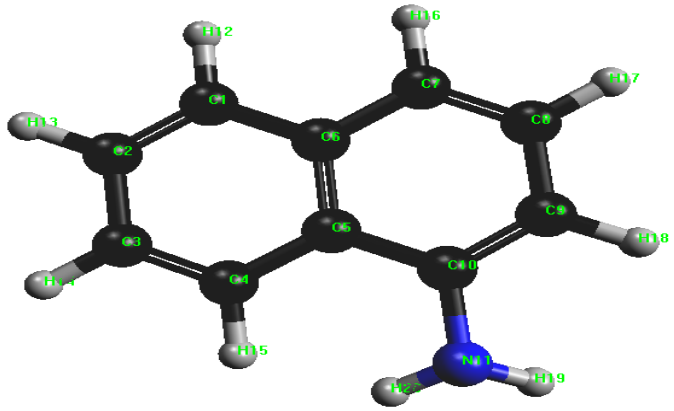

Fig. 4. A: Optimized geometry of NA.

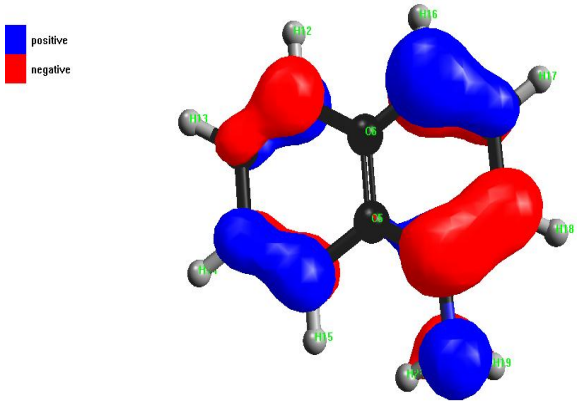

Fig. 4, B: HOMO distribution.

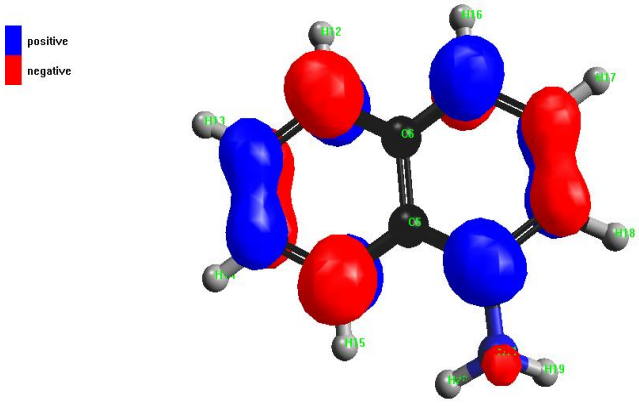

Fig. 4, C: LUMO distribution.

Table 3 Quantum chemical parameters of NA.

E_{HOMO} (eV)	E_{LUMO} (eV)	ΔE (eV)	Dipole moment, μ (debye)
-8.211	-0.378	7.833	35.12

Table 4 Mulliken atomic charges for NA.

no	atom	charge	no	atom	charge
1	C	-0.1782	11	N	-0.0091
2	C	-0.1860	12	H	0.1943
3	C	-0.1913	13	H	0.1921
4	C	-0.1721	14	H	0.1924
5	C	-0.0628	15	H	0.1849
6	C	-0.0168	16	H	0.1961
7	C	-0.2122	17	H	0.1886
8	C	-0.1516	18	H	0.2002
9	C	-0.2506	19	H	0.0757
10	C	-0.0670	20	H	0.0732

Conclusion

The corrosion of Cu – Ni alloy in 5% HCl was increased with both temperature and acid motion, and decreased with inhibitor concentration. The protection effect of inhibitor was due to formation of physical monolayer on metal surface. The corrosion reaction was controlled by both hydrogen evolution reaction and oxygen reduction. Mathematical modeling was used to fitting the corrosion rate data. The both suggested polynomial and exponential models represent the data successfully with correlation coefficients.

Acknowledgement

This work was supported by Baghdad University, Chemical Engineering Department, which is gratefully acknowledged. Also, special thanks to Prof. Dr. Apprael S. Yaro for his continuous support.

References

1. Trabanelli G., *Corrosion*, 47 (1991) 410.
2. Abdulwahab M., Kasim A., Fayomi O. I., Asuke F., Popoola A. P. I. *J. Mater. Environ. Sci*. 3 (2012) 1177.
3. Al-Luaibi Salah S., Azad Seta, Taobi Abdel-Amir H. *J. Mater. Environ. Sci.* 2 (2011) 148.
4. El bribri A., Tabyaoui M., El Attari H., Boumhara K., Siniti M., Tabyaoui B. *J. Mater. Environ. Sci.* 2 (2011) 156.
5. Bentiss F., Traisnel M., Gengembre L., Lagrenée M. *Appl. Surf. Sci.* 161(2000) 194.
6. Cruz J., Martnez R., Genesca J., Garcea-Ochoa E. *J. Electroanal. Chem.* 566 (2004) 111.
7. Wahdan M.H., Gomma G.K., *Mater. Chem. Phys.* 47 (1997) 176.
8. Abdennaby A.M.S., Abdulhady A.I., Abu-Oribi S.T., Saricimen H. *Corros. Sci*. 38 (1996) 1791.
9. E.M. Sherif, S.M. Park, Electrochim. Acta 51 (2006) 4665.
10. Ehteshamzade M., Shahrabi T., Hosseini M.G. *Appl. Surf. Sci*. 252 (2006) 2949.
11. Khadom A. A., Yaro A. S., Kadum A A H., *J. Taiw. Ins. Chem. Eng*. 41 (2010) 122.
12. David H., Modern Analytical Chemistry, McGraw-Hill Companies, USA, (2000).
13. Matos J.B., . Pereira L.P, Agostinho S.M.L., Barcia O.E., Cordeiro G.O., D'Elia E. *J. Electroanal. Chem.* 570 (2004) 91.
14. Popova A., Sokolova E., Raicheva S., Christov M. *Corros. Sci.* 45 (2003) 33.
15. Khadom A. A., Yaro A. S., Abdul Amir H.K., AlTaie A. S., Musa A. Y., *Am. J. Appl. Sci.* 6 (2009) 1403.
16. Poornima T., Jagannath Nayak , Shetty A. N. *Corros. Sci.* 53 (2011) 3688.

17. Khadom A. A, Yaro A. S., AlTaie A. S., Kadum A. A. H. *Portugaliae Electrochimica Acta* 27 (2009) 699.
18. Yaro A. S., Khadom A. A., Ibraheem H. F. *Anti – Corros. Meth. Mater.* 58 (2011) 116.
19. Khadom A. A., Yaro A. S., A. H. Kadhum, *J Chil. Chem. Soc.*, 55 (2010) 150-152.
20. Ahmed Abdel Nazeer, A., Fouda, A.S., Ashour, E.A. *J. Mater. Environ. Sci.* 2 (2011) 24.
21. Wei-hua Li, Qiao He, Sheng-tao Zhang, Chang-ling Pei, Bao-rong Hou. *J. Appl. Electrochem.* 38 (2008) 289.
22. Ashassi-Sorkhabi H., Shaabani B., Seifzadeh D. *Appl. Surf. Sci.* 239 (2005) 154.
23. Moretti G., Guidi F., Grion G. *Corros. Sci.* 46 (2004) 387.
24. Shams E1 Din A.M., E1 Dahshan M.E., Taj El Din A.M. *Desalination* 130 (2000) 89.
25. D. Tromans, Silva J.C. *J. Electrochem. Soc.* 143 (1996) 458.
26. Zhang D.Q., Gao L.X., Zhou G.D. *Corros. Sci*. 46 (2004) 3031.
27. Stupnisek-Lisac E., Brnada A., Mance A.D. *Corros. Sci*. 42 (2000) 243.
28. Sherif E.M., Park S.M. *Electrochim. Acta* 51 (2006) 6556.
29. Ma H., Chen S., Niu L., Zhao S., Li S., Li D. *J. Appl. Electrochem.* 32 (2002) 65.
30. Kear G., Barker B.D., Walsh F.C. *Corros. Sci*. 46 (2004) 109.
31. Martinez S., Tagljar I. *J. Mol. Struct*. 640 (2003) 167.
32. Bereket G., Hur E., Özşahin Ç. *J. Mol. Struct.* 578 (2002) 79.
33. Ma H., Chen S., Liu Z., Sun Y. *J. Mol. Struct.: Theochem.* 774 (2006) 19.
34. Gao G., Liang C. *Electrochim. Acta* 52 (2007) 4554.
35. Lebrini M., Lagrenée M., Traisnel M., Gengembre L., Vezin H., Bentiss F. *Appl. Surf. Sci*. 253 (2007) 9267.
36. Kraka E., Cremer D. *J. Am. Chem. Soc.* 122 (2000) 8245.
37. Gece G. *Corros. Sci*. 50 (2008) 2981.

(2013) ; http://www.jmaterenvironsci.com